Dependence of Copper Species on the Nature of the Support for Dispersed CuO Catalysts

Antonella Gervasini*

Dipartimento di Chimica Fisica ed Elettrochimica & Centro di Eccellenza CIMAINA, Università degli Studi di Milano, via C. Golgi 19, 20133 Milano, Italy

Maela Manzoli and Gianmario Martra

Dipartimento di Chimica I.F.M. & NIS Centre of Excellence, Università di Torino, via P. Giuria 7, I-10125 Torino, Italy, and UdR Torino 1 Interuniversity Consortium INCA

Alessandro Ponti

Istituto di Scienze e Tecnologie Molecolari, Consiglio Nazionale delle Ricerche, via Golgi 19, I-20133 Milano, Italy, and UdR Milano Università, INSTM, via Giusti 9, 50121 Firenze, Italy

Nicoletta Ravasio* and Laura Sordelli

Istituto di Scienze e Tecnologie Molecolari, Consiglio Nazionale delle Ricerche, via Golgi 19, I-20133 Milano, Italy

Federica Zaccheria

Dipartimento di Chimica Inorganica, Metallorganica e Analitica (CIMA), Università degli Studi di Milano, via Venezian 21, I-20133 Milano, Italy

Received: November 15, 2005; In Final Form: February 20, 2006

Copper catalysts prepared by chemisorption−hydrolysis technique over silica (Cu/Si) and silica−alumina (Cu/SiAl) supports were studied to understand the role of the support on the nature and surface properties of the copper species stabilized on their surfaces. The morphological and surface properties of the copper phases have been characterized by complementary techniques, such as HRTEM, EXAFS-XANES, EPR, XPS, and FTIR. For the FTIR investigation, molecular probes (CO and NO) were also adsorbed on the surfaces to test the reactivity of the copper species. Moreover, the catalytic performances of the two catalysts have been compared in the HC−SCR reaction (NO reduction by C_2H_4) performed in highly oxidant conditions. The superior activity and selectivity of the supported silica−alumina catalyst with respect to that supported on silica could be related with the different nature of the copper species stabilized on the two supports, as emerged from the results obtained from the spectroscopic investigations. Small and well-dispersed CuO particles were present on silica, whereas isolated copper ions predominated on silica−alumina, likely in regions rich in alumina that made some exchangeable sites available, as indicated by FTIR spectra of adsorbed CO. The less positive global charge of copper species on Cu/SiAl than in Cu/Si has been confirmed by EPR, XPS, and EXAFS-XANES analyses.

Introduction

In the past few years, the number of patents and scientific papers dealing with the use or the preparation of copper catalysts has been growing continuously. This is mainly due to the activity and the selectivity exhibited by these catalysts in a wide series of reactions suitable to be used, on one hand, in pollutants abatement processes, such as the direct decomposition of NO[1−3] and the selective lean reduction of NO_x to N_2 by hydrocarbons in excess of O_2,[4,5] and, on the other hand, in hydrogenation or oxidative coupling in liquid media.[6,7]

However, the activity in some of these reactions needs to be improved. Copper dispersion, depending in turn from the catalyst preparation method, has been shown to be one of the key factors for the catalytic activity.[8−10]

That is why we focused our attention on the chemisorption−hydrolysis technique, allowing a higher dispersion of the metallic phase in supported copper catalysts. By comparing two sets of Cu/TiO_2 samples with copper loading ranging from 2 to 8%, one obtained by the conventional wet impregnation technique and the other by the so-called "chemisorption−hydrolysis" method, some of us found that samples obtained with the latter technique show much higher Cu(0) specific surface areas. Moreover, we could show that on both samples, highly dispersed two-dimensional (2D) copper aggregates rendered partially electropositive by interaction with the support are present, whereas small and well-dispersed three-dimensional (3D) copper metallic particles are only present on samples prepared by chemisorption−hydrolysis.[11]

The same morphological and surface properties of the copper phase were also found on Cu/SiO_2 and two $Cu/SiO_2−TiO_2$

* To whom correspondence should be addressed. E-mail: antonella.gervasini@unimi.it (A.G.), n.ravasio@istm.cnr.it (N.R.).

10.1021/jp056604c CCC: $30.25
Published on Web 03/25/2006

TABLE 1: Textural Features and Characteristics of Supports and Catalysts

	Cu (wt %)	SSA_{BET} ($m^2 \cdot g^{-1}$)	PV ($mL \cdot g^{-1}$)	RP_{av} (Å)
SiO_2		313	1.79	114
Cu/Si	8.2	332	1.06	64
$SiO_2-Al_2O_3$	–	485	0.79	33
Cu/SiAl	8.7	412	0.75	37

samples prepared by chemisorption−hydrolysis.[12] In particular, every sample was found to contain both 3D and platelike 2D metal particles. From these results, showing that the metallic phase is essentially the same on both a nonporous semiconductor oxide like pyrogenic TiO_2 and on a porous insulating oxide like SiO_2, we draw the conclusion that the features of the supported phase produced following the adopted preparation and activation methods do not depend on the nature of the carrier.

When we moved to a very different material as the support, namely a commercial $SiO_2-Al_2O_3$ cogel containing 13 wt % of Al_2O_3, we soon found a dramatic difference in the spectroscopic features that urged us to deeply investigate the new material obtained. In this paper, we will present its characterization by HRTEM, XANES, EPR, XPS, and FTIR.

For the sake of comparison, the previously reported TEM and FTIR characterization of a Cu/SiO_2 sample with the same metal loading (8 wt %) and prepared by the same technique[12] was completed with EXAFS, EPR, and XPS techniques. The activity of the two oxide catalysts in the selective catalytic reaction of NO_x by hydrocarbons in the excess of oxygen (hereafter indicated as HC−SCR) will be discussed in light of the differences observed.

Experimental Section

Materials. $Cu/SiO_2-Al_2O_3$, hereafter referred to as Cu/SiAl, was prepared by what was called in previous papers[11,12] chemisorption−hydrolysis. The support was a silica−allumina cogel from Grace Davison (Worms, D) containing ca. 13 wt % of Al_2O_3. Such a powder was added to a $Cu(NH_3)_4^{2+}$ solution prepared by dropping aqueous NH_3 to a $Cu(NO_3)_2 \cdot 3H_2O$ solution until pH = 9. After 20 min under stirring, the slurry, held in an ice bath at 273 K, was diluted to allow hydrolysis of the copper complex and deposition of the finely dispersed product to occurr. Under these conditions, no dissolution of the support was detected. The solid was separated by filtration, washed with water, dried overnight at 383 K, and calcined in air at 673 K for 4 h.

As a reference material, a Cu/SiO_2 catalyst, hereafter referred to as Cu/Si, was considered. This catalyst was the subject of a previous study.[12] Relevant surface and textural properties of the samples, BET specific surface area, pore volume calculated by the BJH method,[13] and average pore radius determined by Gurvitsh rule are listed in Table 1.

High purity gases (Praxair) were employed in the activation treatments and in adsorption experiments related to IR measurements. In particular, O_2 and CO were used without any further purification except liquid nitrogen trapping, whereas NO was freshly distilled before use, and its purity was checked by mass analysis.

Methods. *TEM* measurements were made with a JEOL 2000EX electron microscope, equipped with a polar piece and a top entry stage. The powder was ultrasonically dispersed in isopropyl alcohol, and a drop of the suspension was deposited on a copper grid covered with a lacey carbon film.

EXAFS. Cu K edge extended X-ray adsorption fine-structure (EXAFS) and near-edge X-ray adsorption structure (XANES) measurements were carried out in transmission mode at the XAS-13 beamline of the DCI ring at LURE (Orsay, France), using a Si(111) channel-cut and Si(311) double-crystal monochromator, respectively. EXAFS spectra, recorded over an energy range of 1 keV and a sampling step of 1 eV, have been acquired at least three times to perform the statistical analysis and to increase the signal-to-noise ratio by averaging the extracted EXAFS oscillations. XANES spectra have been recorded with a resolution of 0.5 eV.

The samples were loaded inside the BN sample holders, which are part of the Little-type transmission cell for in situ treatments under controlled temperature and gas flow. The samples have been measured in both EXAFS and XANES modes at ambient temperature after each one of the following treatments: (a) calcination ex situ and hydration in air; (b) in situ oxidation in O_2 flow at 543 K; (c) in situ reduction at 543 K.

The oxidized samples have been loaded in air inside the Little-type transmission EXAFS-cell for in situ treatments under controlled temperature and gas flow and reduced in situ in a 10 mL/min H_2 flow at 543 K for 1 h. The spectra have been recorded at ambient temperature in flowing N_2.

EXAFS data analysis was performed with the program developed by Michalowicz.[14] A copper metal foil was used as reference for the Cu−Cu contributions, and CuO and Cu_2O were used for the Cu−O contributions. Experimental phase and amplitude functions have been calculated from the back-Fourier transformed filtered peaks of the references sample spectra. Phase and amplitude functions for each pair have been also calculated with the FEFF7 program[15] for several distances. For the metallic pairs, the program gives a good agreement with the experimental functions.

The spectra have been analyzed in the typical k range from 2.7 to 12.7 $Å^{-1}$. The R intervals for the peak extraction are indicated for every sample. The best fits of the extracted $k^3\chi(k)$ signals of the filtered back-transformed peaks were determined by a least-squares spherical curve-fitting procedure, where the maximum parameter number is determined by the expression $N_{par} < 2\Delta k \Delta R/\pi + 2$.[16] The parameter error bars were calculated from the experimental standard deviation derived from the averaging of the extracted $\chi(k)$ function.[17] The F test[18] was applied when necessary to distinguish between fits of similar quality.

EPR. As for the EPR measurements, the calcined Cu/Si and Cu/SiAl catalysts were placed in 4 mm o.d. quartz tubes. Spectra were recorded by means of a Bruker Elexsys X-band spectrometer equipped with a Bruker ER4111VT variable temperature unit. Typical conditions are: microwave frequency ca. 9.4 GHz, microwave power 20 mW (10 dB), magnetic field sweep range 200 mT (1024 points), modulation frequency 100 kHz, modulation amplitude 0.5 mT, sweep time 84 s. Spectra were taken at temperatures between 115 and 298 K (±1 K). The magnetic field was measured with a Bruker ER036TM teslameter; the microwave frequency was measured by a Hewlett-Packard HP 5340A frequency counter.

Experimental spectra were fitted to a spectral model with the following characteristics: electron Zeeman and copper hyperfine interactions are assumed to be axial and mutually coaxial. The presence of both copper isotopes ^{63}Cu and ^{65}Cu (relative abundance 69.2:30.8) was taken into account. The amplitude of the homogeneous line is computed by averaging the square of the transition matrix element over all directions perpendicular

to the static field. The width of the homogeneous line is affected by both crystallite orientation and correlation of the *g*- and *A*-strain.[19]

XPS. The surfaces of Cu/Si and Cu/SiAl catalysts were examined by X-ray photoelectron spectroscopy (XPS), collecting the spectra by an M-Probe apparatus (Surface Science Instruments). The X-ray source provided monochromatic Al Kα radiation (1486.60 eV). The residual pressure in the analysis chamber was typically 5×10^{-9} Torr. Charge effects were compensated by the use of a flood gun (3 eV). A spot size of 400 μm × 1000 μm and a pass energy of 150 eV were used for survey spectra, whereas for the single-region acquisitions a spot size of 200 μm × 750 μm and a pass energy of 25 eV with 0.74 eV resolution were used. The Si 2p line from silica (103.3 eV) was used as an internal reference with an accuracy of ±0.20 eV. The quantitative analysis was performed using the sensitivity factors given by Scofield [20] from the intensities of Cu $2p_{3/2}$, Si 2s, and Al 2p. The XPS peaks were decomposed using a peak-fitting routine. The lines used in the fitting of a peak envelope are defined according to their centered position, half-width, shape (Gaussian or Lorentzian distribution), and intensity. The best fit of the experimental curve by a tentative combination of bands was searched.

IR Spectra were recorded at room temperature (r.t.) in an infrared cell designed to treat the samples in situ, using a Perkin-Elmer FTIR 1760 spectrometer at a resolution of 2 cm^{-1}; the number of scans (100−200) was varied according to the transmission of the sample, with the aim to obtain similar levels of noise. Before the measurements, the samples were submitted to a thermal treatment in O_2 at 673 K (oxidized samples) followed by an outgassing from the same temperature down to r.t. The spectra of adsorbed NO and CO are reported in Absorbance, after subtraction of the spectrum of the samples before gas admission. Band integration and curve fitting have been carried out by "Curvefit", in Spectra Calc (Galactic Industries Co.) by means of Lorentzian curves.

Catalytic Tests. The catalytic activity in the SCR of NO_x by C_2H_4 (HC−SCR reaction) in excess oxygen was measured in a flow apparatus at atmospheric pressure. The fixed-bed quartz tubular down flow microreactor was filled with ca. 0.5 g of catalyst, sieved as particles 0.25−0.35 mm in size, and mounted in a tube furnace heated by a temperature controller (from Eurotherm) able to realize automatically programmed thermal sequences and isothermal steps. Before the test, the catalyst sample was activated at 623 K in He stream for 4 h (5.5 $NL \cdot h^{-1}$).

The reaction was studied at temperatures between 423 and 773 K; each examined temperature was maintained for 200 min; meanwhile, four chromatographic analyses were performed. The reaction temperature was then increased (10 °C min^{-1}) to the successive one, without intermediate activation. The overall test lasted about 35 h. Reaction feed consisted of 0.4% of both NO and C_2H_4 and 4% of O_2 with He as balance. Typically, the mixture flowed at 5.5 $NL \cdot h^{-1}$, which corresponded to a space velocity of about 8000 h^{-1}. The reactor outflow was analyzed by gas chromatography (C. P. 9000 from Chrompack) equipped with T. C. D. detector. A 60/80 Carboxen-1000 column (Supelchem) permitted the separation of N_2, O_2, NO, N_2O, CO, CO_2, and C_2H_4. Reaction selectivity to the main product, N_2, was evaluated by means of the competitiveness factor (cf., %), defined as the ratio between the amount of C_2H_4 consumed to reduce NO to N_2 and the total amount of C_2H_4 consumed.[21,22]

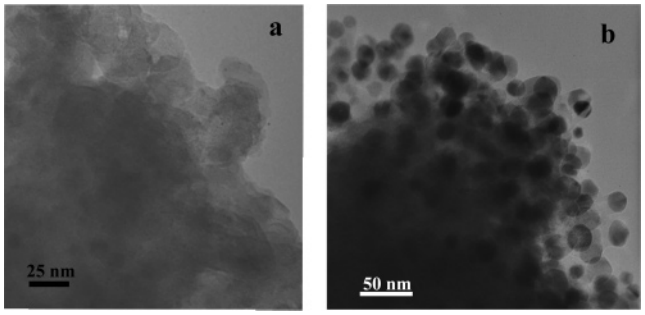

Figure 1. (a) TEM image of a region where initially no supported particles are observed (original magnification: ×400 000). (b) After 5 min exposure to the electron beam in the same region (original magnification: ×200 000).

Results and Discussion

TEM. TEM inspection of the calcined $Cu/SiO_2-Al_2O_3$ catalyst evidenced some heterogeneity in the dispersion of copper on the support. Only a few $SiO_2-Al_2O_3$ grains presented on their surfaces well-defined, supported particles of ca. 5.0 nm in size, whereas for the overwhelming part of the sample, no evidence for supported particles was obtained, even at higher magnification (Figure 1a). However, after a few minutes of exposure to the electron beam, a number of supported particles with size in the 10−20 nm range appeared also in these regions (Figure 1b). This behavior witnesses for the presence of oxidized copper species highly dispersed on the support, initially not detectable by TEM, which are reduced to the metal state by interaction with the electrons of the beam and aggregate to form metal particles, as also observed in a previous study on Cu/TiO_2 catalyst.[11]

On the contrary, on both Cu/SiO_2 and Cu/SiO_2-TiO_2 calcined systems, small particles, well distributed all over the carriers, with a size distribution over the 2.0−5.5 nm range, were observed.[12]

EXAFS-XANES. Preliminarly Cu K edge EXAFS spectra of the sample Cu/Si have been measured as a reference for the novel Cu/SiAl supported system. In Figure 2 the comparison of the Fourier transformed spectra at the Cu K edge of the Cu/Si and Cu/SiAl samples is reported, and in Table 2, the results of the best fit procedures are reported.

The Fourier transformed EXAFS spectrum of the freshly calcined Cu/SiAl sample (thick line in Figure 2A) exhibits only one main peak fitted by six oxygen atoms at 1.939 Å. A small contribution at about 3.0 Å could eventually be fitted by less than one Cu atom, but the absence of the outer shells characteristic of CuO aggregates proves that by interaction with SiO_2/Al_2O_3, the copper atoms are dispersed on the surface as isolated ions or, at least, as vicinal atoms in Cu−O−Cu species. The spectroscopic features of this species are almost coincident with those reported by Prestipino et al. for a surface copper aluminate phase in alumina supported $CuCl_2$ catalyst.[23]

Conversly, the Cu/Si catalyst calcined in oxygen at 543 K (thin line in Figure 2A) shows the contribution of about six oxygen atoms detected at 1.947 Å and a large peak corresponding to about five Cu atoms at an average Cu−Cu distance of 2.987 Å. By comparing the EXAFS results with the copper oxide crystallographic data, it appears that on silica, CuO-like oxidic aggregates, with no oxide crystallyne order, are formed as proved by the relevant contribution of next nearest Cu neighbors at the Cu−Cu distance not corresponding to the second shell of crystal CuO.

Interestingly, the Cu/Si sample shows the same shell structure around the copper atoms as before calcination, that is, when it

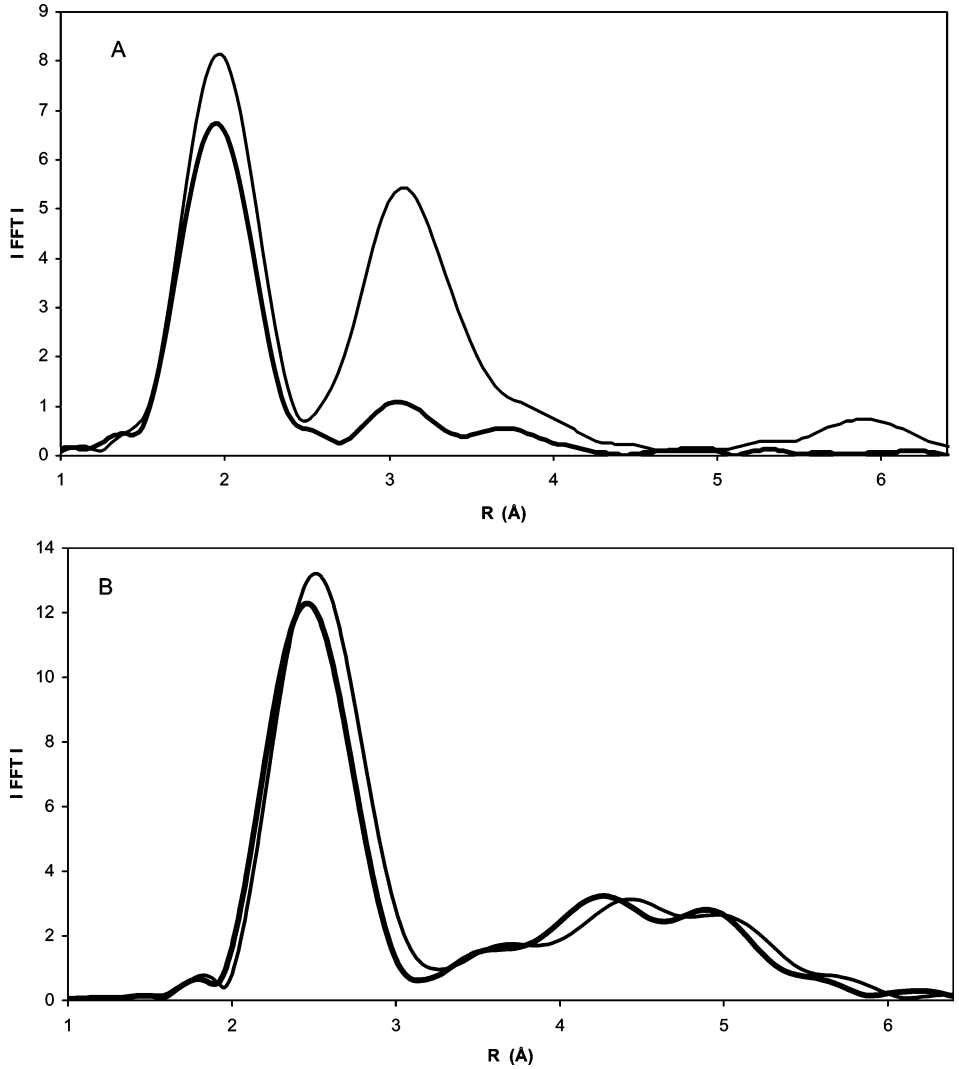

Figure 2. Cu K edge Fourier transformed EXAFS spectra of catalysts: (A) calcined at 543 K: Cu/Si (solid line), Cu/SiAl (thick line); (B) in situ reduced under H_2 flow at 543 K: Cu/Si (solid line), Cu/SiAl (thick line).

TABLE 2: Curve Fitting Results of the Cu K edge EXAFS Data

sample	treatment	shell	CN	R (Å)	σ_{DW} (Å)	ΔE_0 (eV)
Cu/Si	O_2	O	6.0 + 0.2	1.947 + 0.002	0.079 + 0.003	1.7 + 0.2
		Cu	4.8 + 0.2	2.987 + 0.002	0.091 + 0.003	6.6 + 0.2
Cu/SiAl	O_2	O	6.0 + 0.3	1.939 + 0.002	0.095 + 0.002	1.5 + 0.2
Cu/Si	in situ H_2	Cu	7.9 + 0.3	2.547 + 0.002	0.084 + 0.001	−1.3 + 0.1
Cu/SiAl	in situ H_2	Cu	7.8 + 0.3	2.571 + 0.002	0.092 + 0.002	−11.1 + 0.2
Cu/SiAl	in situ H_2 at 673 K	Cu	8.9 + 0.3	2.555 + 0.002	0.076 + 0.002	0.2 + 0.2

is just prepared (after washing and drying treatment), where an hydroxyde gel is expected. This suggests the presence of an oxidic amorphous phase on the calcined catalyst.

In Figure 2B, the comparison of the Fourier transformed Cu K edge spectra, corrected for the Cu phase, of the two samples after in situ reduction at 543 K is reported. The Cu/Si spectrum shows a single large peak, whose back-transformed filter fit gives 7.9 Cu atoms at 2.547 Å (Table 2). The inclusion of a possible O contribution from the support does not reproduce a statistically more significant fit. The overall spectrum strongly resembles that of the Cu metal foil with its characteristic fcc fingerprint from the outer shells. The first-shell Cu−Cu distance is slightly smaller than in the Cu foil (2.556 Å), as expected for relatively small particles, and the disorder parameters corresponds to the theoretical r.t. crystal value, suggesting that there is no significant contribution from the structural disorder.

The spectrum of Cu/SiAl after the in situ reduction treatment in flowing hydrogen at 543 K (thick line in Figure 2B) shows the presence of the Cu contribution only, with a first shell of 7.9 neighbors at 2.571 Å. These values, together with the trend of the next shells, suggest that on the SiAl support, copper is present as small metal particles with fcc structures. However, the best fit of the in situ reduced Cu/SiAl sample gives a $\Delta E_0 = -11$ eV, which is quite high for metal copper and suggests an electron-poor character of the metal particles. Only after a further in situ reduction at 673 K a value of ΔE_0 close to 0, diagnostic of a true metallic character, can be obtained. These particles clearly cannot be formed through reduction of the aluminate-like phase that requires much higher reduction temperatures, but likely they originate from the very small fraction of CuO in strong interaction with aluminum (vide infra).

The XANES spectra of Cu/Si and Cu/SiAl (Figure 3) are almost coincident and the edge jumps located at an energy value characteristic of Cu(II). However, the spectra are completely

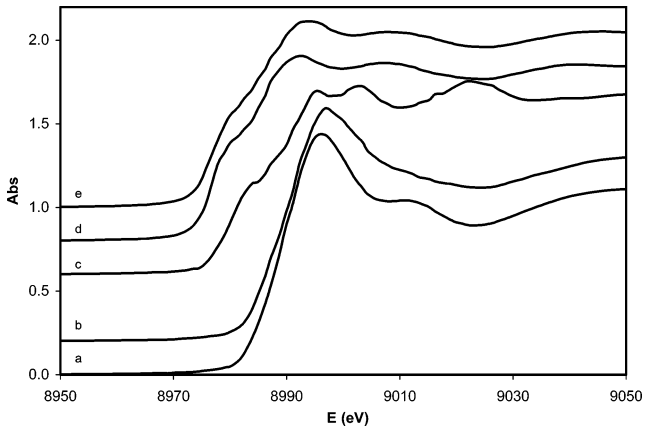

Figure 3. Cu K edge XANES spectra of (a) Cu/Si and (b) Cu/SiAl catalysts calcined at 543 K, together with reference spectra of (c) Cu foil, (d) Cu_2O, and (e) CuO.

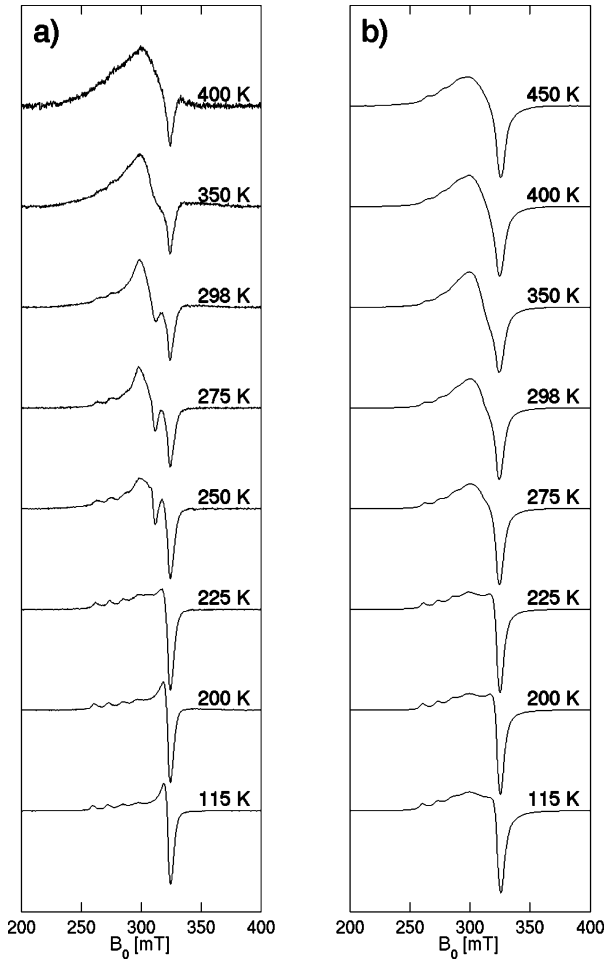

Figure 4. EPR spectra of (a) Cu/Si and (b) Cu/SiAl catalysts as a function of recording temperature. For the sake of clarity, each spectrum has been individually scaled to unit amplitude.

different from those of both CuO and Cu_2O (considered as references for Cu(II) and Cu(I) species). The absence of any pre-edge structure suggests a distorted octahedral coordination geometry, as reported for Cu ions in zeolites,[24,25] where two O's belong to the support surface and two O's belong to OH groups. Two axial water molecules at longer distances complete the coordination sphere.

EPR. The EPR spectra of catalysts Cu/Si and Cu/SiAl are reported as a function of temperature in Figure 4. All spectra can be interpreted as the superposition of at least two subspectra. The first subspectrum (labeled L, for low temperature) can be seen in almost pure form in the spectrum at 115 K for Cu/Si. It is the typical spectrum of isolated Cu(II) ions in a (quasi)axial environment, with $g_{\|} > g_{\perp}$ and resolved features due to hyperfine coupling to the copper nucleus ($I = 3/2$) in the parallel region (260−300 mT). In the perpendicular region, about 330 mT, hyperfine splitting is not resolved because it is much smaller than in the parallel region and because of the presence of off-axis peaks.[26] Accurate g values and hyperfine couplings for this subspectrum could be obtained by spectral simulation as detailed below. The second subspectrum (labeled H, for high temperature) can be seen in almost pure form in the spectrum at 400 K of Cu/Si. It is a distorted axial spectrum without resolved hyperfine splittings, although its magnetic field span is comparable to that of L. From the high-temperature spectra, it can be estimated that the species corresponding to the H subspectrum has $g_{\|} \cong 2.25$ and $g_{\perp} \cong 2.08$ in Cu/Si and $g_{\|} \cong 2.25$ and $g_{\perp} \cong 2.09$ in Cu/SiAl. In this case, the absence of hyperfine splitting in H is the result of dipolar and/or exchange interaction between Cu(II) ions. The third subspectrum (J) is only observed at temperatures between 250 and 350 K in Cu/Si. Like H, subspectrum J has no resolved hyperfine splittings, but it is much narrower, extending from 290 to 315 mT.

Subtraction of H spectrum from the total spectrum aided to discern that subspectrum J has $g_{\|} \cong 2.25$ and $g_{\perp} \cong 2.17$ at 250 K, and that it quickly becomes isotropic upon heating ($g \cong 2.19$ at 298 K). Moreover, subtraction of H spectrum allowed us to obtain a very good simulation of the subspectrum L at 155 K, as shown in Figure 5a. The spin Hamiltonian parameters of subspectrum L in Cu/Si at 155 K are: $g_{\|} = 2.408$, $g_{\perp} = 2.085$, $A_{\|} = 137 \times 10^{-4}$ cm^{-1}, $A_{\perp} < 10 \times 10^{-4}$ cm^{-1}. Estimated error in g is ± 0.002 and in A is $\pm 2 \times 10^{-4}$ cm^{-1}. The EPR spectrum of the Cu/SiAl catalyst suffers from extensive overlap of subspectra L and H at all temperatures between 115 and 450 K (Figure 4b). We observed a transformation of the L subspectrum into the H subspectrum on raising temperature, a behavior already reported in the literature.[27] An accurate simulation of the well-resolved L subspectrum could be obtained by subtracting the spectrum recorded at 450 K from that obtained at 115 K (Figure 5b). The spin Hamiltonian parameters of subspectrum L in Cu/SiAl at 155 K are: $g_{\|} = 2.392$, $g_{\perp} = 2.088$, $A_{\|} = 146 \times 10^{-4}$ cm^{-1}, $A_{\|} < 20 \times 10^{-4}$ cm^{-1}, with estimated errors as above.

Isolated Cu(II) ion species have received a great deal of attention from EPR spectroscopists; $g_{\|}-A_{\|}$ correlation diagrams, first proposed by Peisach and Blumberg,[28,29] are useful to rationalize the experimental data. Plotting the present results onto such diagram, one can see that both spectra (Cu/Si and Cu/SiAl) arise from Cu(II) ions with four oxygen ligands in the equatorial positions. More interestingly, the spin Hamiltonian parameters of Cu(II) ions in the Cu/Si catalyst are typical of copper complexes with an overall charge of +2, whereas those of copper in the Cu/SiAl catalyst are typical of copper complexes with an overall charge of +1.

Trouillet et al.[30] recently studied Cu(II) complexes supported on silica during the preparation of catalysts similar to the Cu/Si catalyst dealt with in the present work. After calcination and exposure to air, they observed a spectrum with $g_{\|} = 2.382$, $g_{\perp} = 2.069$, $A_{\|} = 136 \times 10^{-4}$ cm^{-1} and attributed it to a Cu(II) ion coordinated to four water molecules and to two $-O^-$ singly charged oxygen atoms at the silica surface, also on the basis of previous EXAFS experiments. Although their g values are about 0.02 lower than ours, the two species are probably very similar as the $A_{\|}$ values coincide. However, on the basis of the

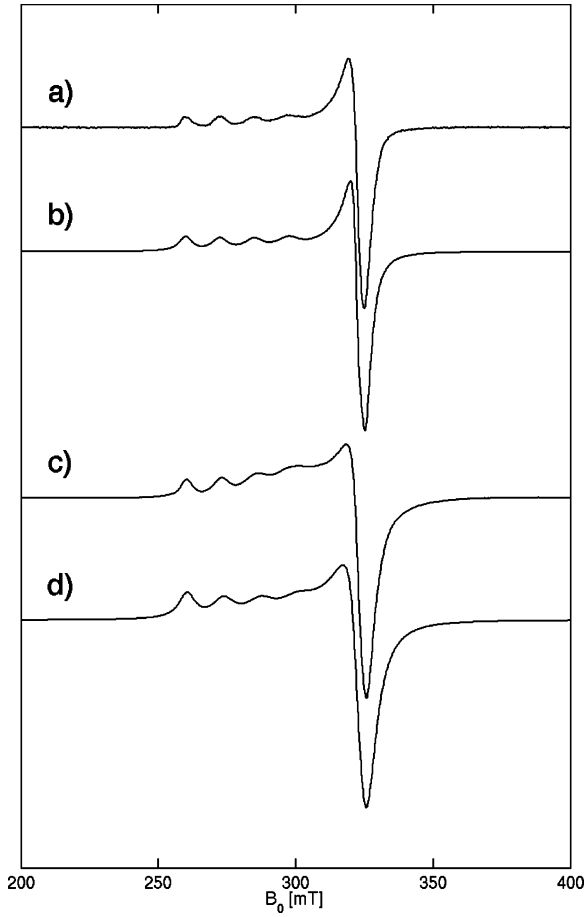

Figure 5. Simulation of low-temperature EPR spectra of catalysts Cu/Si and Cu/SiAl after subtraction of the correspondent high-temperature spectra (almost pure subspectra L are thus obtained). (a) Difference of experimental spectra of Cu/Si taken at 115 and 400 K; (b) simulated subspectrum L of Cu/Si (see text for parameters); (c) difference of experimental spectra of Cu/SiAl taken at 115 and 450 K; (d) simulated subspectrum L of Cu/SiAl (see text for parameters).

correlation diagram, it seems that the copper complex in the Cu/Si catalyst may be better described as coordinated to two neutral −OH groups at the silica surface, in addition to four water molecules, so that the overall charge of the complex is +2.

The Cu(II) ions in Cu/SiAl have a coordination sphere similar to those in Cu/Si but with a less positive global charge. Copper(II) complexes supported on alumina have also been studied.[31,32] Catalysts with a copper content similar to Cu/SiAl had EPR spectra very similar in shape to those in Figure 4b and $g_{||}$ and $A_{||}$ values typical of an overall neutral complex. It was concluded that the Cu(II) ions in Cu/SiAl are in an intermediate situation between those found in silica and alumina. The distorted axial subspectrum H with no resolved hyperfine interaction to the copper nucleus has been observed many times in systems similar to Cu/Si and Cu/SiAl. Various authors observed that such a subspectrum becomes relatively larger as the copper loading on the sample is increased.[31−33] Therefore, subspectrum H was attributed to a static clustering of copper ions. On the other hand, the presently observed transformation of the L subspectrum into H subspectrum on raising temperature, a behavior already reported in the literature,[27] hints at a dynamical phenomenon related to collisions or temporary aggregation of copper complexes and, thus, to the mobility of copper on the catalyst surface. Under this respect, the Cu/Si and Cu/SiAl catalysts are very different. In Cu/Si there is only minor static clustering at low temperature and copper mobility is large enough that at 400 K subspectrum L vanishes. Conversely, in Cu/SiAl static copper aggregation is important, maybe because of preferential clustering in alumina rich regions, but mobility is much lower than in Cu/Si because the L subspectrum is clearly discernible even at 450 K.

XPS. The XP spectra of the Cu/Si and Cu/SiAl surfaces in the 968−924 eV region are reported in Figures 6 and 7. The intense and broad photoelectron peak at about 934 eV (Cu $2p_{3/2}$) observed for the two Cu-based catalysts are in agreement with numerous reports of copper oxide systems supported on different oxidic phases. However, the difficulty in discriminating between Cu(II) or Cu(I) is well-known when there is a copresence of the two species at the surface, as the binding energy values are similar (i.e., 933.6 and 932.5 eV for CuO and Cu_2O, respectively). In this case, not only the binding energy values but also other typical features of the XPS spectrum can help in the assignment.

An important difference between the XPS spectra of the two samples is the shape of the Cu 2p peaks. The XP spectrum of Cu/SiAl presents only one contribution in the Cu $2p_{3/2}$ band (Cu $2p_{3/2}$, 933.15 eV), whereas Cu/Si presents two contributions to the Cu 2p peaks (Cu $2p_{3/2}$, 932.9 and 935.3 eV), indicating for this sample the existence of two Cu(II) species with different valence states. Typically, CuO species are observed at 933.6 eV, and the shift at higher binding energy is indicative of a charge transfer from the metal ion toward the support oxide.[34] Córdoba et al.[35] observed an analogous shift in the XPS spectra of CuO/TiO_2 samples in which dispersed CuO species (933 eV) and those of −Cu−O−Ti−O− (935 eV) have been recognized. In the present case, for the Cu/Si system, the presence of well dispersed Cu(II) interacting with the −OH groups of the silica support (935.3 eV) could be inferred, besides CuO species.

A second important difference between the XP spectra of Cu/SiAl if compared with that of Cu/Si is related to the presence of Cu 2p satellite peaks. It is known that the main XPS characteristic for Cu(II) species are the appearance of spin−orbit split Cu $2p_{1/2}$ and Cu $2p_{3/2}$ peaks along with their shake-up satellites.[35−38] The satellites are well evident only for Cu/Si, with an intensity ratio of the satellite to the corresponding principal peak (I_{sat}/I_{pp}) close to 0.5. Conversely, the satellite peaks could only be guessed for Cu/SiAl. The absence of satellite peaks or very low values of the I_{sat}/I_{pp} ratio observed for Cu/SiAl suggest the presence of Cu(I) or copper species in lower valence state than those present on the Cu/Si.

As regards the copper dispersion of the two samples, information could derive from the surface Cu, Si, and Al concentrations (expressed as atomic %) obtained by integration of the Cu $2p_{3/2}$, Si 2s, and Al 2p peaks, respectively. By comparing the molar ratios between the Cu, Si, and Al surface species, ($Cu_{2p}/(Si_{2s})$ or $Cu_{2p}/(Si_{2s}+Al_{2p})$), and the total metal species, (Cu/Si or Cu/(Si+Al), obtained from ICP), for the two samples, respectively, values near 1 for Cu/Si and 0.35 for Cu/SiAl were found. Values near 1 indicate that the Cu concentration at the surface is comparable with that calculated from total molar ratios. On the contrary, values lower than 1 indicate that the surface is less concentrated in Cu than that one could calculate on the basis of the total molar ratio. The lower amount of surface copper on Cu/SiAl than on Cu/Si can justify some degree of Cu clustering and/or entrapment within the pores in the alumina-rich region of the silica−alumina support.

IR Spectra of Adsorbed Probe Molecules. *Preliminary Remarks on Cu/Si.* The study on the Cu/Si catalyst previously carried out allowed to conclude, on the basis of TEM and diffuse

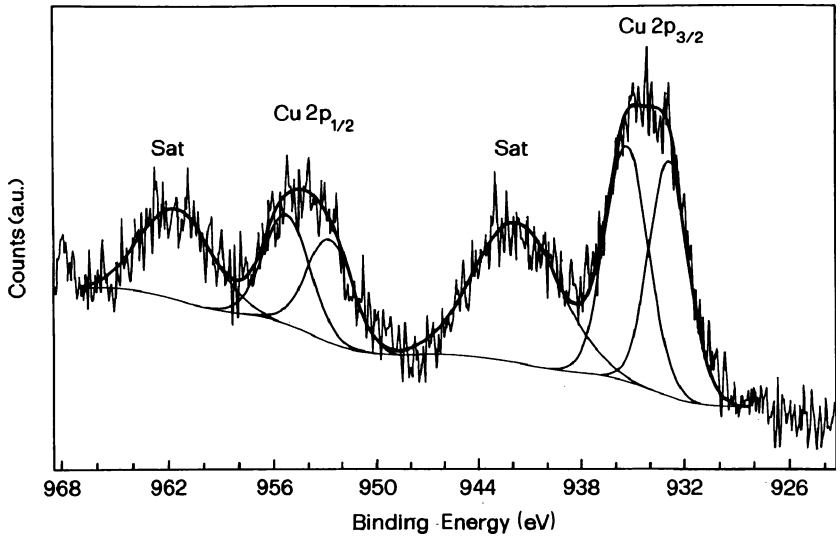

Figure 6. XPS spectrum of Cu 2p core level of the calcined Cu/Si catalyst.

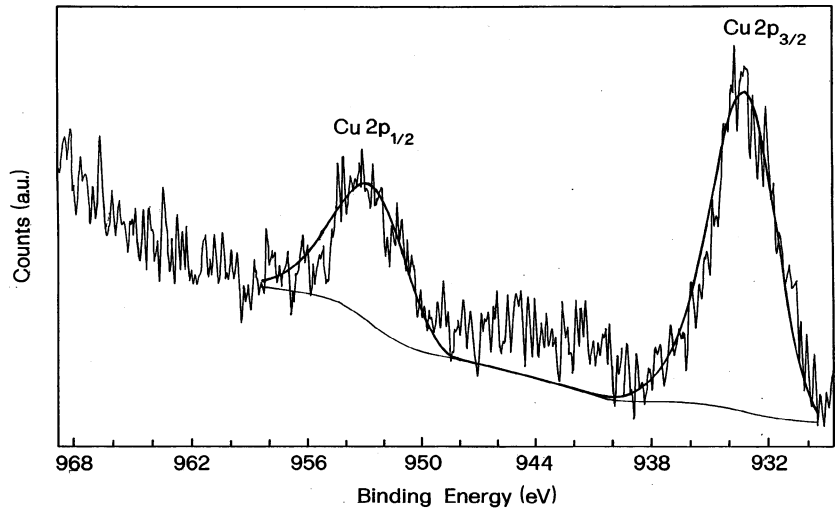

Figure 7. XPS spectrum of Cu 2p core level of the calcined Cu/SiAl catalyst.

reflectance UV−vis data, that after calcination copper was essentially present as Cu_xO ($x = 1,2$) particles, although no highly dispersed copper ions should have been present.[12] For this reason, the characterization of the materials in the calcined form by IR spectroscopy of adsorbed probe molecules was not of interest, also because the calcined material was only the precursor of the catalyst actually active in the investigated reaction (oxidative coupling of 2,6-dimethylphenol) only after reduction.[7]

On the other hand, the IR spectra of CO adsorbed on Cu/Si treated in H_2 in mild conditions (523 K) revealed the presence of copper only as 3D and platelike 2D metal particles, the latter rendered partially electropositive by interaction with surface oxygen atoms of the support.[12]

IR Spectra of NO Adsorbed on Cu/SiAl. The IR spectra of NO adsorbed at r.t. on the oxidized Cu/SiAl sample are shown in Figure 8. In the presence of 8 mbar NO, a quite intense and symmetric band at 1904 cm^{-1} is produced, accompanied by a weaker component at 1813 cm^{-1} (Figure 8a). By decreasing the NO pressure, the main band significantly decreases in intensity, without shifting in position (Figure 8b−e), but a residual fraction is left after outgassing (Figure 8f), corresponding to NO molecules irreversibly adsorbed at r.t. At the same time, the minor band at 1813 cm^{-1} decreases in intensity by decreasing the NO pressure and finally disappears after outgassing.

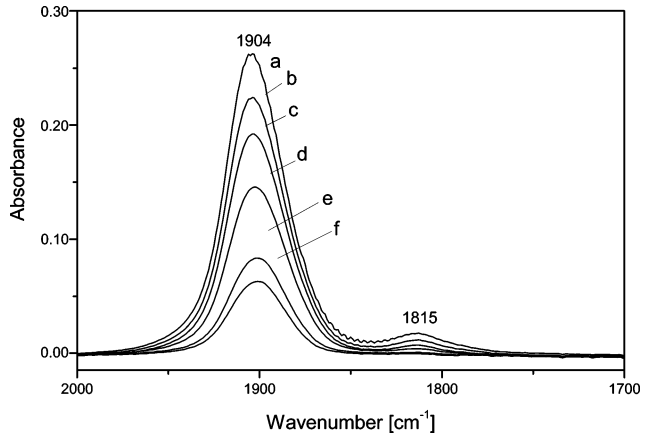

Figure 8. IR spectra of the oxidized Cu/SiAl sample collected in the presence of: (a) 8, (b) 2, (c) 0.5, (d) 0.08 mbar NO and after (e) 30 s and (f) 10 min outgassing at the same temperature.

On the basis of such behavior and of literature data dealing with copper in zeolites,[39] the band at 1904 cm^{-1} can be assigned to NO adsorbed on isolated Cu(II) sites, whereas the 1813 cm^{-1}

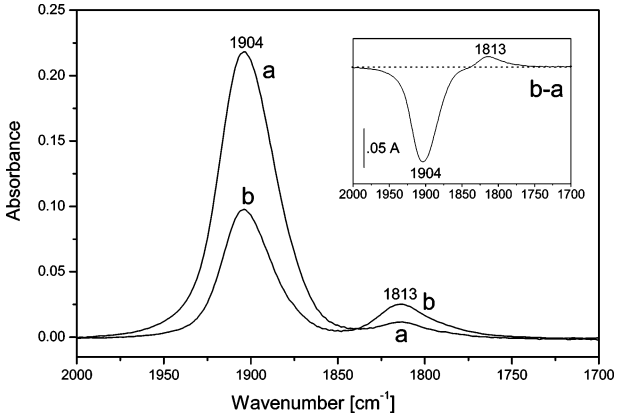

Figure 9. IR spectra of 1.4 mbar of NO adsorbed at r.t. on the oxidized (curve a) and on the reduced (curve b) Cu/SiAl sample. (Inset) Difference between spectrum (b) and spectrum (a).

one, which is fully reversible, can be associated to NO adsorbed on copper sites with a lower oxidation state, likely Cu(I).[40] The previous assignment was further confirmed by adsorbing 1.4 mbar NO on a Cu/SiAl sample reduced by treatment in H_2 at 523 K. The obtained spectrum, compared with the equivalent related to NO adsorbed on the calcined sample, is reported in Figure 9. It can be observed that by turning from the oxidized (Figure 9a) to the reduced (Figure 9b) sample, the band at 1904 cm^{-1}, due to Cu(II)−NO adducts, appears significantly less intense, whereas that at 1813 cm^{-1}, related to Cu(I)−NO species exhibits a higher intensity. Such a comparison allowed us to estimate the relative amount of Cu ions in the two oxidation states in the two samples. In fact, by assuming that for each Cu(II) a single Cu(I) species is produced, the decrease in intensity of the band at 1904 cm^{-1} and the related increase in intensity of that at 1813 cm^{-1} should correspond to the conversion of a certain amount of Cu(II)−NO adduct into an equal number of Cu(I)−NO species. Such decrease and increase in intensity have been quantified by subtracting spectrum a from spectrum b in Figure 9 (result in the inset) and calculating the integrated absorbance of the components obtained in this way.

As the number of NO oscillators related to each component in the difference spectrum is the same, the ratio between their integrated areas corresponds to the ratio between the extinction coefficients (ϵ) of the ν_{NO} mode of NO adsorbed on Cu(II) and on Cu(I) sites. The obtained result is $[\epsilon(\nu_{NO-Cu(II)})/\epsilon(\nu_{NO-Cu(I)})] = 11.25$. Now, turning to the spectra of NO adsorbed on the oxidized sample (Figure 9a) and on the reduced one (Figure 9b), taking into consideration the Lambert−Beer Law (with the same optical path), the following expression can be written for both samples:

$$I_{1904}/I_{1813} = [\epsilon(\nu_{NO-Cu(II)})/\epsilon(\nu_{NO-Cu(I)})] \times (C_{Cu(II)}/C_{Cu(I)}) \quad (1)$$

where I_{1904}/I_{1813} is the ratio between the integrated intensities of the bands at 1904 cm^{-1} and at 1813 cm^{-1} for each sample and $C_{Cu(II)}/C_{Cu(I)}$ is the relative amount of Cu(II) and Cu(I) sites. The numerical values for the oxidized and reduced samples are reported in Table 3. The results indicate that even in the Cu/SiAl oxidized sample, the Cu(I) ions are present in a not negligible relative amount and became largely predominant after reduction in hydrogen at 523 K.

IR Spectra of CO Adsorbed on Cu/SiAl. *Oxidized Cu/SiAl.* The adsorption of 20 mbar CO at r.t. on the oxidized Cu/SiAl sample produced in the carbonyl stretching region a main band at 2158 cm^{-1}, slightly asymmetric on the low-frequency side and with a shoulder at 2183 cm^{-1}, and a weak band at 2208

TABLE 3: Integrated Intensities (I) of the ν_{NO} Bands at 1904 and 1813 cm^{-1}, Relative Extinction Coefficients (ϵ) and Amount of Cu(II) and Cu(I) Derived from the Analysis of the Difference Spectrum in the Inset of Figure 9 for Cu/SiAl

pretreatment	I_{1904}	I_{1813}	I_{1904}/I_{1813}	$\epsilon(\nu_{NO-Cu(II)})/\epsilon(\nu_{NO-Cu(I)})$	$C_{Cu(II)}/C_{Cu(I)}$
oxidation at 673 K	8.89	0.23	38.65	11.25	3.4
reduction at 523 K	3.53	0.71	4.97	11.25	0.4

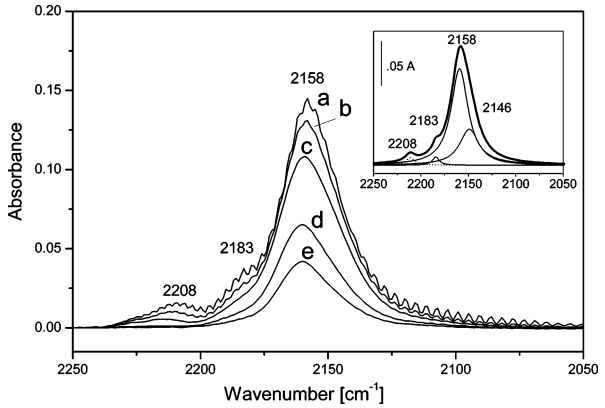

Figure 10. IR spectra of the oxidized Cu/SiAl sample collected at r.t. in the presence of: (a) 20, (b) 5, (c) 0.5 mbar CO and after (d) 30 s and (e) 20 min outgassing at the same temperature. (Inset) Curve fitting of spectrum (a) in the mainframe.

cm^{-1} (Figure 10a). As reported in the inset, the curvefitting of the experimental spectrum (a) revealed that the asymmetry on the low-frequency side of the 2158 cm^{-1} band is actually due to a weak component at 2146 cm^{-1}. By decreasing the CO pressure (Figure 10b−d) and outgassing 1 h at r.t. (curve e), the band at 2208 cm^{-1} and the two components at 2183 and 2146 cm^{-1} disappear. On the contrary, the band at 2158 cm^{-1} undergoes a strong decrease in intensity but does not disappear. The weak band at 2208 cm^{-1} is straightforwardly assigned to CO adsorbed on low-coordinated Al^{3+} sites.[41] As CO is not adsorbed on Cu(II) at r.t., the other components should be related to CO adsorbed on Cu(I) sites. In particular, a band around 2160 cm^{-1} was observed for monocarbonyl adduct on Cu(I) ions in zeolites.[40−43] Furthermore, the two minor components at 2183 and 2146 cm^{-1} are similar in position to those due to geminal dicarbonyls on Cu(I).[40] These features indicate that in our Cu/SiAl material, the Cu(I) ions are stabilized on the silica−alumina islands with a small fraction of Cu(I) sites with a coordinative unsaturation high enough to adsorb two CO molecules. However, it must be considered that the adsorption of CO on copper ions in +1 oxidation state is irreversible under outgassing at r.t.[44,45] By contrast, the band at 2158 cm^{-1} observed for CO on Cu/SiAl is largely reversible in this condition. Such a feature suggests that a fraction of the copper ions, identified as Cu(I) until now, should actually be $Cu^{\delta+}$ ions, with $1 < \delta < 2$, the lower electron density with respect to true Cu(I) ions affecting the energy of the interaction. On the other hand, part of the 2158 cm^{-1} band resisting to outgassing (Figure 10e) corresponds to CO on Cu(I) sites.

The heterogeneity in the electronic features of copper ions in the low-oxidation state revealed by CO poses a question about the interaction with NO discussed above. In fact, the different interaction strength exhibited by $Cu^{\delta+}$ ($1 < \delta < 2$) with respect to Cu(I) toward CO could occur also toward NO. If this is the case, the band at 1813 cm^{-1} observed in the spectra of adsorbed NO, completely reversible by outgassing at r.t. (Figure 8), could be due to: (i) the interaction with the stronger $Cu^{\delta+}$ ($1 < \delta < 2$) sites only, being Cu(I) ions too weak as adsorbing

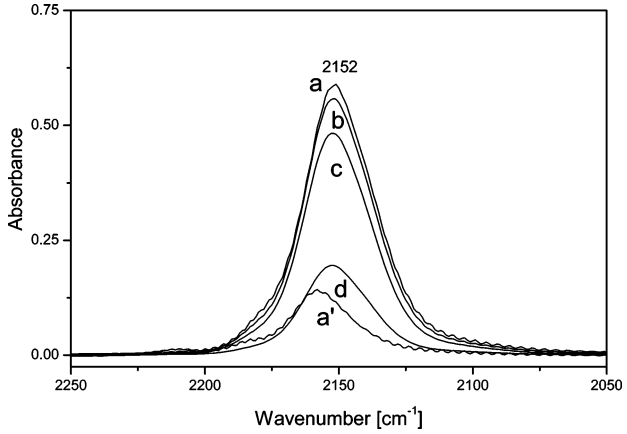

Figure 11. IR spectra of the "used" Cu/SiAl sample collected at r.t. in the presence of: (a) 20, (b) 5, (c) 0.5 mbar CO and after (d) 20 min outgassing at the same temperature compared with (a′) the IR spectrum of the "fresh" CuSiAl sample in the presence of 20 mbar CO.

centers for NO; (ii) the interaction with both Cu(I) and $Cu^{\delta+}$ ($1 < \delta < 2$) sites, the difference in the strength of interaction with the two kind of sites being too small to produce some discontinuity in the progressive decrease in intensity exhibited by the 1813 cm^{-1} band upon outgassing. As a consequence, the relative amount of copper ions in low oxidation state, calculated as in Table 3, in case (i) should correspond to the relative amount of Cu(I) only, whereas in case (ii) should correspond to the relative amount of (Cu(I) + $Cu^{\delta+}$) with respect to Cu(II).

Cu/SiAl after HC−SCR Reaction in Model Conditions. CO adsorption was also performed on the Cu/SiAl catalyst after HC−SCR reaction carried out at 523 K in model, batch condition in the FTIR cell and followed by outgassing at the same temperature, resulting in the complete removal from the surface of molecular species related to the reaction (as checked by IR, spectra not shown). The IR spectra obtained by contacting the so-treated catalyst with CO are reported in Figure 11 (curves a−d) compared with that recorded at full CO coverage before and after the reaction (Figure 11a′).

It can be noticed that for the "used" catalyst, a spectral pattern similar in shape and slightly downshifted with respect to that related to CO on the "fresh" one, but with a significant higher intensity, is obtained. Such a behavior indicates that, despite the presence of oxygen, at least in the adopted model conditions, the HC−SCR reaction has a reducing effect on the copper sites, transforming a part of Cu(II) (not evidenced by CO at r.t.) into Cu at a lower oxidation state. Moreover, the large but not complete reversibility of the 2152 cm^{-1} band observed by decreasing the CO pressure and subsequent outgassing indicates that both $Cu^{\delta+}$ ($1 < \delta < 2$) and Cu(I) sites are produced by such a reduction process.

Catalytic HC−SCR Reaction. The catalytic performances of CuO on pure or modified siliceous supports have been already presented in the literature.[46] Concerning the comparison between the two catalysts at similar CuO content but differently supported, Cu/Si and Cu/SiAl, details are here reported. The maximum NO reduction conversion to N_2 was about 30 and 40% for Cu/Si and Cu/SiAl, respectively (553−573 K). For higher temperatures, N_2 formation decreased, leading to a typical volcano-shaped curve for the NO conversion−temperature curves. Selectivity, in terms of competitiveness factor (cf., %), decreased as temperature increased for both the catalysts, as the C_2H_4 oxidation by O_2 prevailed on C_2H_4 oxidation by NO. At low temperatures (<523 K), Cu/SiAl showed the highest cf. value. The differences between the Cu/Si and Cu/SiAl catalysts in terms of activity and selectivity in the SCR are depicted in Figure 12. In this representation, the C_2H_4 conversion can be regarded as an index of the extent of reaction, because it can be oxidized by NO or by O_2, leading in any case to carbon oxides. C_2H_4 conversion increased with temperature and attained 100% conversion at temperature around 623 K in any case. For given C_2H_4 conversion, higher N_2 formation was always observed on Cu/SiAl than on Cu/Si; this leads to a higher NO−C_2H_4 curve than that of Cu/Si.

Considering the experimental data obtained up to the increasing NO conversion with temperature, specific integral reaction rates (r) could be calculated and expressed as $mol_{N2} \cdot mol_{Cu} \cdot s^{-1}$, once the amount of Cu per unit mass of catalyst is known. In this calculation, r values coincide with turnover frequencies, assuming that all the Cu introduced into the catalyst coincide with the active sites. If this hypothesis cannot hold, r values are underestimated when calculated as turnover frequency values. This would be the case for Cu/SiAl rather than for Cu/Si, the fraction of copper exposed at the surface being lower (see XPS paragraph). Figure 13 shows the linear trends obtained by plotting ln r as a function of inverse temperature in a

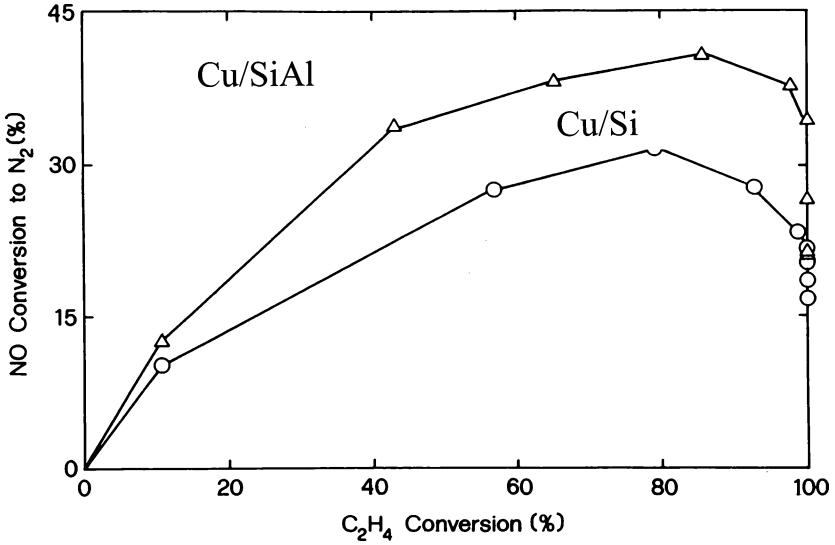

Figure 12. Conversion of NO to N_2 as a function of CO_2 produced during the SCR reaction by C_2H_4 in oxidizing atmosphere over the two Cu catalysts. Each marker corresponds to different reaction temperatures in the 423−773 K temperature range.

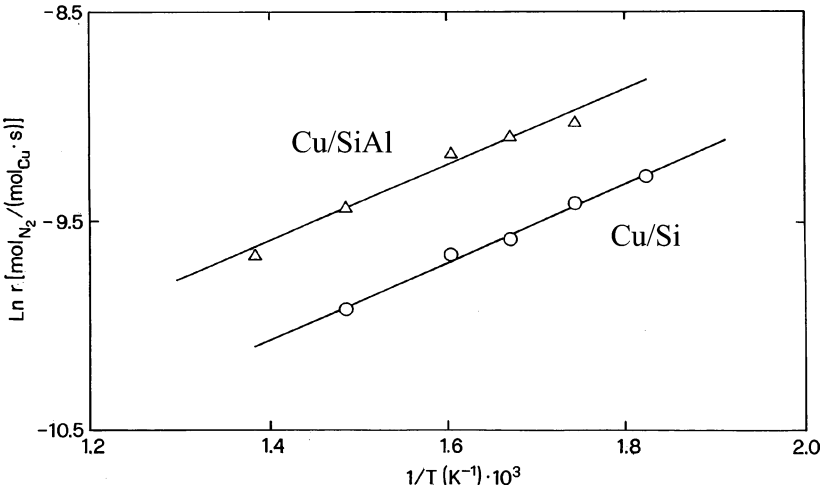

Figure 13. Arrhenius-like plot for the NO conversion to N_2 in the SCR reaction by C_2H_4 in oxidizing atmosphere over the two Cu catalysts.

Arrhenius-like plot, for the two catalysts. Both trends are satisfactorily linear in the temperature domain investigated. The lines are well apart from each other, and the highest *r* values are associated with Cu/SiAl catalyst, as expected, it being the most active one. As the amount of Cu is similar in the two catalysts whereas the concentration of Cu is higher on the Cu/Si surface than on Cu/SiAl, one can argue that the active copper sites on the surface of Cu/SiAl have a much higher turnover frequency for NO conversion to N_2 than those present on Cu/Si.

Besides the important catalytic role played by the highly dispersed CuO phase, as recognized in the literature,[8−10] isolated copper species, stabilized by the acidic support, can give account for the observed higher activity. When the SCR activity of Cu−oxide systems is compared with that of Cu−zeolites, the higher activity of the latter can be ascribed to the higher number of isolated copper centers that are stabilized in exchange positions of the zeolitic lattice. On Cu−MFI catalysts,[48] although there are different copper environments, isolated copper ions are recognized the most active species for SCR of NO.

Conclusions

The collection of results obtained in this study indicated that the deposition of copper by using the same "chemisorption−hydrolysis" method resulted in different supported species if silica or silica−alumina were employed as support. In fact, on SiO_2, small and well-dispersed CuO particles are produced after calcination, converted in metallic Cu small particles by reduction in H_2, whereas on $SiO_2-Al_2O_3$ mainly isolated copper ions, likely belonging to a surface Cu−aluminate-like phase and strongly resistant to reduction, are obtained. Only from TEM and EXAFS results can the presence of a well-dispersed CuO-like phase reducible to the metallic state be inferred as expected by bulk techniques, which do not discriminate between surface and embedded contributions. However, this phase represents only a very small fraction of the copper exposed, whereas isolated $Cu^{\delta+}$ ($1 \leq \delta \leq 2$) species phase give account of almost all the surface metal.

The main features of the Cu−aluminate-like phase, as emerged from all the spectroscopic techniques used (EXAFS, EPR, XPS, and IR of adsorbed NO and CO), are (i) the presence at the surface, after oxidative treatment, of isolated copper species with oxidation state ranging from (II) to (I), with a significant decrease in the amount of the Cu(II) species in favor of $Cu^{\delta+}$ ($1 < \delta < 2$) and Cu(I) ones after reduction, and (ii) a high resistance to a further reduction to the zerovalent state, with a consequent very limited production of metal particles. The nature of this particular silica−alumina support, very different from those previously studied by some of us,[11,12] may be responsible for the presence of this copper species. Thus, the total number of acidic sites and particularly the number of strong acid sites of this silica alumina material determined by adsorption calorimetry are close to those determined for a H−Beta zeolite sample.[47] This shows that on the surface of this support, exchangeable sites are available, in analogy with zeolitic materials. The exchange with the $Cu(NH_3)_4^{2+}$ solution then generates isolated copper species, hardly reducible to an oxidation state lower than monovalent copper, as put in the evidence by all the techniques used throughout this paper. Kuroda[25] already showed that the existence of Brønsted acid sites on the surface of various supports is an important factor in determining the state of copper ions in the supported catalysts.

On the contrary, none of the supports previously studied, namely TiO_2, SiO_2, and mixed SiO_2-TiO_2, possess strong acid sites. For these materials, the presence of a highly dispersed CuO-like phase was ascribed to the difference between the pH of the $Cu(NH_3)_4^{2+}$ solution and the surface zero-charge point.[8]

As far as the catalytic activity is concerned, in our previous studies on a series of Cu catalysts supported on silica and modified silicas, we ascribed the catalytic activity to the preparation method allowing to obtain a high dispersion of the CuO like phase.[46] In the present case, the catalytic activity may well be due to the presence of the partially reduced copper phase. On the other hand, the detailed characterization of this sample, where the support is a silica alumina with a 13% content in Al_2O_3, brought new evidences on the role played by the support in determining the surface metallic phase and in turn its catalytic activity.

Acknowledgment. We acknowledge the support and the use of the facility of the LURE synchrotron laboratory in Orsay (Paris) and thank the staff of the XAS-13 beamline for their assistance. M.M. and G.M. acknowledge the Interuniversity Consortium "Chemistry for the Environment"- INCA for financial support (Project "Urban Atmosphere"). We all thank Professor Flora Boccuzzi, University of Torino, for helpful discussions.

References and Notes

(1) Dandekar, A.; Vannice, M. A. *Appl. Catal., B* **1999**, *22*, 179.

(2) Wang, X.; Hou, W.; Wang, X.; Yan, Q. *Appl. Catal., B* **2002**, *35*, 185.

(3) Liu, Z.; Amiridis, M. D.; Chen, Y. *J. Phys. Chem. B* **2005**, *109*, 1251.
(4) Shelef, M. *Chem. Rev.* **1995**, *95*, 209.
(5) Pârvulescu, V. I.; Grange, P.; Delmon, B. *Catal. Today* **1998**, *46*, 233.
(6) Boccuzzi, F.; Chiorino, A.; Gargano, M.; Ravasio, N. *J. Catal.* **1997**, *165*, 140.
(7) Boccuzzi, F.; Martra, G.; Partipilo Papalia, C.; Ravasio, N. *J. Catal.* **1999**, *186*, 327.
(8) Praliaud, H.; Mikhailenko, S.; Chajar, Z.; Primet, M. *Appl. Catal., B* **1998**, *6*, 359.
(9) Indovina, V.; Occhiuzzi, M.; Pietrogiacomi, D.; Tuti, S. *J. Phys. Chem. B* **1999**, *103*, 9967.
(10) Márquez-Alvarez, C.; Rodríguez-Ramos, I.; Guerrero-Ruiz, A.; Haller, G. L.; Fernandéz-García, M. *J. Am. Chem. Soc.* **1997**, *119*, 2905.
(11) Boccuzzi, F.; Chiorino, A.; Martra, G.; Gargano, M.; Ravasio, N.; Carrozzini, B. *J. Catal.* **1997**, *165*, 129.
(12) Boccuzzi, F.; Coluccia, S.; Martra, G.; Ravasio, N. *J. Catal.* **1999**, *184*, 316.
(13) Lowell, S.; Shields, J. E. *Powder Surface Area and Porosity*; Scarlett, B., Ed.; Powder Technology Series; Chapman and Hall: London, 1984.
(14) Michalowicz, A. *J. Phys. IV*, **1997**, 7C2−235.
(15) Zabinsky, S. J.; Rehr, J. J.; Ankunikov, A.; Albers, R. C.; Eller, M. J. *Phys. Rev. B* **1995**, *52*, 2995.
(16) Lengeler, B.; Eisenberger, E. P. *Phys. Rev. B: Condens. Matter Mater. Phys.* **1980**, *21*, 4507.
(17) Report of the International Workshop on Standards and Criteria in XAFS. In *X-ray Absorption Fine Structure*; Hasnain, S. S., Ed.; Hellis Horwood: Chichester, NY, 1991; p 751.
(18) Joyner, R. W.; Martin, K. H.; Meehan, P. *J. Phys. C: Solid State Phys.* **1987**, *20*, 4005.
(19) Carl, P. J.; Larsen, S. C. *J. Phys. Chem. B* **2000**, *104*, 6568.
(20) Scofield, J. H. *J. Elect. Spectrosc. Relat. Phenom.* **1976**, *8*, 129.
(21) Bethke, K. A.; Kung, M. C.; Yang, B.; Shah, M.; Alt, D.; Li, C.; Kung, H. H. *Catal. Today* **1995**, *26*, 169.
(22) Gervasini, A.; Carniti, P.; Ragaini, V. *Appl. Catal., B* **1999**, *22*, 201.
(23) Prestipino, C.; Bordiga, S.; Lamberti, C.; Vidotto, S.; Garilli, M.; Cremaschi, B.; Marsella, A.; Leofanti, G.; Fisicaro, P.; Spoto, G.; Zecchina, A. *J. Phys. Chem. B* **2003**, *107*, 5022
(24) Kuroda, Y., Kumashiro, R., Nagao, M., *Appl. Surf. Sci.* **2002**, *196*, 408
(25) Kuroda, Y., Mori, T., Yoshikawa, Y., Kittaka, S., Kumashiro, R., Nagao, M., *Phys. Chem. Chem. Phys.* **1999**, *1*, 3807
(26) Ovchinnikov I. V.; Konstantinov, V. N. *J. Magn. Reson.* **1978**, *32*, 179.
(27) Anderson M. W.; Kevan, L. *J. Phys. Chem.* **1987**, *91*, 4174.
(28) Peisach J.; Blumberg, W. E. *Arch. Biochem. Biophys.* **1974**, *165*, 691.
(29) Carl P. J.; Larsen, S. C. *J. Catal.* **1999**, *182*, 208.
(30) Trouillet, L.; Toupance, T.; Villain F.; Louis, C. *Phys. Chem. Chem. Phys.* **2000**, *2*, 2005.
(31) Centi, G.; Perathoner, S.; Biglino D.; Giamello, E. *J. Catal.* **1995**, *151*, 75.
(32) Leofanti, G.; Padovan, M.; Garilli, M.; Carmello, D.; Zecchina, A.; Spoto, G.; Bordiga, S.; Palomino, G. T.; Lamberti, C. *J. Catal.* **2000**, *189*, 91.
(33) Sakata, S.; Nakai, T.; Yahiro H.; Shiotani, M. *Appl. Catal., A* **1997**, *165*, 467.
(34) Auroux, A.; Gervasini, A.; Guimon, C. *J. Phys. Chem. B* **1999**, *103*, 7195.
(35) Córdoba, G.; Viniegra, M.; Fierro, J. L. G.; Padilla, J.; Arroyo, R. J. *Solid State Chem.* **1998**, *138*, 1.
(36) Xu, B.; Dong, L.; Chen, Y. *J. Chem. Soc., Faraday Trans.* **1988**, *94*, 1905.
(37) Espinós, J. P.; Morales, J.; Barranco A.; Caballero, A.; Holgado, J. P.; González-Elipe, A. R. *J. Phys. Chem. B* **2002**, *106*, 6921.
(38) Morales, J.; Caballero, A.; Holgado, J. P.; Espinós, J. P.; González-Elipe, A. R. *J. Phys. Chem. B* **2002**, *106*, 10185.
(39) Giamello, E.; Murphy, D.; Magnacca, G.; Shioya, Y.; Nomura, T.; Anpo, M. *J. Catal.* **1992**, *136*, 510.
(40) Spoto, G.; Zecchina, A.; Ricchiardi, G.; Martra, G.; Leofanti, G.; Petrini, G. *Appl. Catal. B* **1994**, *3*, 151.
(41) Morterra, C.; Magnacca, G. *Catal. Today* **1996**, *27*, 497, and references therein.
(42) Huang, Y. *J. Am. Chem. Soc.* **1973**, *95*, 6636.
(43) Iwamoto, M.; Yahiro, H.; Tanda, K.; Mizumo, N.; Mine, Y.; Kagawa, S. *J. Phys. Chem.* **1991**, *95*, 3727.
(44) Padley, M. B.; Rochester, C. H.; Hutchings, G. J.; King, F. *J. Chem. Soc., Faraday Trans.* **1994**, *90*, 203.
(45) Millar, G. J.; Rochester, C. H.; Waugh, K. C. *J. Chem. Soc., Faraday Trans.* **1991**, *87*, 1467.
(46) Carniti, P.; Gervasini, A.; Modica, V. H.; Ravasio, N. *Appl. Catal., B* **2000**, *28*, 175.
(47) Dragoi, B.; Gervasini, A.; Dumitriu, E.; Auroux, A. *Thermochim. Acta* **2004**, *420*, 127.
(48) Torre-Abreu, C.; Ribeiro, M. F.; Henriques, C.; Ribeiro, F. R. *Appl. Catal., B* **1997**, *11*, 383−401.